European Geothermal Congress 2013
Pisa, Italy, 3-7 June 2013

Exploration of geothermally relevant structures in the crystalline basement of Switzerland using gravity constrained by seismic data

Yassine Abdelfettah[1], Eva Schill[2,3]

[1] Laboratory for Geothermics – CREGE, CHYN, University of Neuchâtel, Switzerland

[2] EEIG "Heat Mining", Route de Soultz - BP 40038, F-67250 Kutzenhausen, France

[3] Steinbeis-Transfer Centre "Geoenergy and Reservoir Technology" D-79807 Lottstetten-Nack, Germany

Yassine.abdelfettah@unine.ch

Keywords: Gravity, Butterworth filter, 3D Forward modelling, Finite Element, crystalline basement, Permo-Carboniferous graben.

ABSTRACT

Geothermal heat flow anomalies are often linked to graben structures at the top of the crystalline basement. Numerical thermo-hydraulic models have attributed a strong contribution to fluid flow in the fault zones building up the rim of these through structures. It is, however, a challenge to identify such or any other structures in the crystalline basement. In this paper, we present a 3D geological model based forward modelling employing finite element modelling and a detailed analysis of high- and band-pass Butterworth filters to assess the location and geometry of different geothermally relevant structures in the crystalline basement in Switzerland and elsewhere.

1. INTRODUCTION

Major temperature anomalies in central Europe are found to be linked to hydrothermal advection in fractured crystalline basement (Illies and Greiner 1979; Kohl et al 2000; Pribnow and Schellschmidt 2000; Bächler 2003). Kohl et al (2000) and Bächler (2003) have shown that the convection occurs along fault zones related to the tectonics of the Upper Rhine valley. This convection accounts to about 80% for the temperature anomalies of these geothermal fields (Baillieux et al subm). Along the German-Swiss border, on a length of about 350 km, the heat flux distribution reveals several positive anomalies with up to 160 mW m^{-2} that is comparable to the one observed at the European EGS site at Soultz-sous-Forêts.

Several structural elements in the basement of the Swiss Molasse basin revealing naturally enhanced permeability may contribute to the surface heat flux anomaly pattern (Schill et al., 2012). A 2D thermo-hydraulic modeling for the area of Bad Zurzach (Rybach et al 1987) has revealed a strong influence of deep thermal water up-flow along the Northern boundary fault of late-Variscian graben structures (Permo-Carboniferous troughs) in the granitic basement. Thus, the authors concluded that the heat flux anomaly is related to the occurrence of such Permo-Carboniferous troughs.

These trough structures are complex grabens that extend over tens of kilometers in width. For example, the Northern Swiss trough striking approximately ENE-WSW and extending from E of Basel to the lake of Constance reveals Permian to Stephanian basin fill (Matter et al 1987) and a multiphase tectonic history (Diebold 1989; Diebold and Noack 1997).

A summary of the challenges in the localization of Permo-Carboniferous trough structures using seismic data is given by (Marchant et al., 2005). Seismic interpretation of Permo-Carboniferous (PC) deposits in Switzerland is a challenge that is mainly due to three reasons: (1) in the absence of boreholes, the origin of characteristically weak reflections below the Mesozoic is uncertain, they can be either caused by Paleozoic sediments, shear zones and lithological contrasts within the basement, or alternatively, by seismic artefacts, such as multiples or remnants of reflection point smearing. (2) Where PC deposits are present, the base Mesozoic reflection, which is not always well expressed, can be mistaken for an internal PC reflection, and (3) the structural interpretation is often uncertain, as faults below the Mesozoic cannot be traced along marker horizons on the seismic sections as is the case for the Mesozoic sedimentary layers. These difficulties are illustrated in the seismic atlas of the Swiss Molasse Basin (Sommaruga et al., 2012). In an attempt to better differentiate between reflections originating from Permo-Carboniferous deposits and seismic artefacts, a number of criteria were established on the basis of seismic sections (Marchant et al., 2005). These criteria provide indication which needs to be combined with all other available information in order to establish whether or not PC deposits are present. In this study, we propose to use advanced gravity forward modelling using finite element modelling after analysing residual anomalies using Butterworth filter with different wavelength. We, thus, present here a new numerical code for gravity forward modelling based on 3D geological FE models and a synthetic sensitivity analysis.

2. GEOLOGICAL SETTING

The best investigated trough in Switzerland is the North Swiss trough (Sprecher and Müller, 1986) or Constance – Frick trough (Ustazewski, 2004). In this region, the thickness of Permian sediments in the Upper Rhine Graben was first estimated using seismic and well information as well as paleogeographic considerations (Boigk and Schöneich, 1970, 1974). A first regional interpretation of the gravity data has shown a negative anomaly in the residual field parallel to an axe going southwards through Weiach and Villingen. This anomaly has been interpreted qualitatively in terms of depth of the crystalline basement (Klingelé and Schwendener, 1984). The residual has been obtained by subtracting the regional trend from the Bouguer anomaly, which was determined using a polynomial of third order and fitting their coefficients by least-square. For the interpretation in terms of depth of the top crystalline, the reduction density of 2400 kg m^{-3} has been chosen due to the fact that the areas with PC troughs at depth are overlain by Quaternary sediments with a density close to that value.

Further interpretation has improved the localization of the trough structures mainly using seismic investigation calibrated by well data (Laubscher and Noack, 1997, Diebold et al., 1991, Diebold and Noack, 1997, Pfiffner et al., 1997). The most complete compilation of PC graben structures in northern Switzerland is given in the technical report of Nagra (NAGRA, 2008). A more regional interpretation has also been compiled (Ustazewski, 2004).

In western Switzerland, the seismic interpretation reveals strong faulting at the bottom of the PC troughs (Gorin et al., 1993). The knowledge on the internal structure of the Permo-Carboniferous troughs, however, is limited to a conceptual model of the Constance-Frick trough which is based on borehole data, seismic lines and on the well explored late Paleozoic coal basins in the French Massif Central (Diebold and Noack, 1997).

These structures are found also in the entire crystalline basement of southern Germany including the Upper Rhine graben (Boigk and Schöneich 1974). In this area, however, their contribution to the geothermal potential is mostly unknown.

3. METHODS

Gravity studies have been proven to be a good exploration tool for the investigation of the troughs. It was this method which permitted the first regional interpretation on the extension of the Northern Swiss trough (Klingelé and Schwendener, 1984). Further investigation of gravity to better understand the PC troughs in Switzerland was not employed.

In this study, we have investigated systematically the application of 3D geology for gravity forward modeling using finite elements meshing (FEM) as well as the application of high-pass and band-pass Butterworth filters of different wavelength, to quantify the geometry of PC troughs in the crystalline basement for a representative area of Northern Switzerland.

3.1 Gravity modelling using 3D finite element meshing

In order to assess the possibility of the gravity data to detect and characterize PC troughs in the Molasse basin, 3D synthetic geological models were set up. These models were used to carry out: i) a sensitivity study of the Butterworth filter and ii) a qualitative and quantitative interpretation of these PC grabens. Furthermore, synthetic gravity distributions were generated for different models using a homogeneous basement density of 2670 kg m^{-3}.

The forward modelling is achieved using a finite element code, which is based on the algorithm of Pohanka (1988). The vertical gravity attraction is computed by

$$g(r,\varepsilon) = -G\delta \sum_{k=1}^{K} n_k \sum_{l=1}^{L(k)} \Phi_k \qquad [1]$$

, where

$$\Phi_k = \varphi\left(u_{k,l}(r), v_{k,l}(r), w_{k,l}(r), z_k(r), \varepsilon\right) \qquad [2]$$

and r is the distance between the gravity station and the volume. Further explanations are presented in Pohanka (1988).

The 3D finite element meshing was carried out using the Gmsh (Version 2.5.1, Geuzaine and Remacle 2009). This allows for approaching the geological geometry using tetrahedrons. Gravity stations are located on a real topography and complete Bouguer anomaly was calculated.

3.2 Preferential Butterworth filter

Since in the pre-Alpine basins the Bouguer anomaly is dominated mainly by the gravity effect of the geometry of the Molasse sediments deepening towards the Alps, it needs be corrected for this regional trend to allow for interpretation of the basement structures.

Butterworth filters of different wave length (Abdelfettah and Schill 2012) were applied on the complete Bouguer anomaly to eliminate this trend. This filter is characterized and controlled mainly by two parameters: (1) cut-off frequency (or wavelength) and (2) filter order. The advantage of the Butterworth filter is that we can easily use different wavelength to i) delineate and characterize different negative anomalies at depth, and ii) build a pseudo-tomography using high pass and band pass filter. Depth and size of anomalies are indicated by the wavelength of the filter. With increasing wavelength, we are able to visualize increasing larger or deeper structures. Moreover, the filter order parameter can be changed to delineate a very small variation, for instance, in the

case of low density contrast between the PC trough and the basement. With increasing filter order the horizontal density contrast is emphasized.

4. SENSITIVITY STUDY OF THE BUTTERWORTH FILTER

4.1 Set-up of the FE model

To investigate the power of Butterworth filters with systematic wavelength, a sensitivity study was carried out using a finite element model of and extension of 70×80×10 km. The topography of the model originates from the 25×25 m digital elevation model (DEM) resampled to 1×1 km and reveals minimum and maximum elevation of 173 m and 3020 m.

This model incorporates six 3D volumes at different depth and of different shape representing structural elements expected in the Swiss subsurface (Figure 1). The volumes B1 and B6 represent typical Quaternary deposits in comparably small valleys (B1) and more extended basins (B6) that are expected to provide comparatively short and long wavelengths, respectively. The objective of these two volumes shallower bodies is to investigate if their gravity effects can be removed and distinguished by the filter. The volume B6 is additionally characterized by an eastward dipping bottom and a vertical plane on its eastern boundary. It is mainly used to investigate the differences between deep volumes that are equally expected to cause long wavelengths. Volume B2 may represent a lithological change in the basement such as a crystalline intrusion. Its gravity effect is expected to increase with increasing the wavelength of the filter. Volume B3 represents a structure of small thickness and low angle dip toward west, such as a fault zone. The robustness of the Butterworth filter will be tested on this body. The volumes B4 and B5, two separate bodies, occur on top of each other and at significant but different depth. Their gravity effect is expected to be of large wavelength and to overlap. All these volumes are embedded into a synthetic geological model of the Swiss Molasse basin including the Molasse sediments at the top (Cenozoic), two layers of Mesozoic sediments in the middle, and the crystalline basement at the bottom. A regional dip from north to south is assigned to the Mesozoic sediments causing an increase in thickness of the Cenozoic sediments and thus, fitting the known geology of the Swiss Molasse basin. It should be mentioned that volumes B1 and B6 occur in the Cenozoic formation. B2 to B5 may be found and crosscut different formations down to the basement.

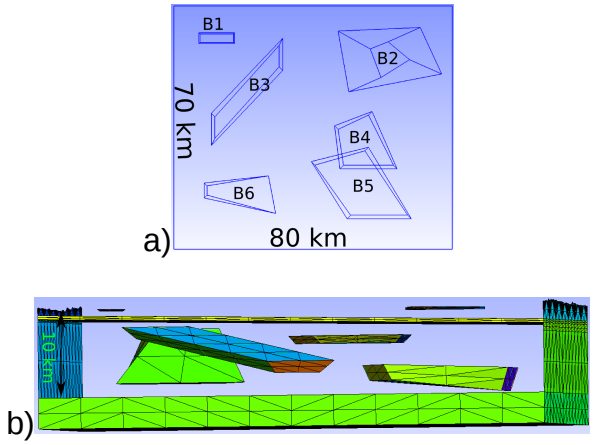

Figure 1: Finite element discretisation of the synthetic 3D geological model used in the sensitivity study of the Butterworth filter showing the geometry and distribution of the investigated volumes B1 to B6 (see in the text) in top view (a) and in a view from the west (b).

For the simulation of Bouguer anomaly, representative density values were attributed to the respective geological units (Table 1). A detailed analysis on this will be described in a forthcoming paper.

Table 1: Density values assigned to the different formations or volumes in 3D geological model (Figure 1) for the sensitivity study of the Butterworth filter.

Formation or volume	Density (kg m^{-3})
Cenozoic (molasses sed.)	2500
Upper Mesozoic	2550
Lower Mesozoic	2600
Crystalline basement	2670
B1	2400
B2	2620
B3	2600
B4	2600
B5	2600
B6	2400

4.2 Bouguer and residual anomalies

Simulation of Bouguer anomaly of the synthetic, geologic 3D FE model is shown in Figure 2 a). As expected from the synthetic geological model, the computed Bouguer anomaly is strongly dominated by the gravity effect of the Molasse sediments. The volumes B1 to B6 appear according to their depth and difference in density to the geological layers as well-outlined anomalies B1 and B6, as significant anomalies such as B2 and B4/B5, or as deformation of the Bouguer isolines B3. Residual anomalies resulting from the application of Butterworth filters of different

type, high and band pass, as well as of different frequencies, 10, 20, 30, 35 and 50 km high pass wavelength, are showed in Figure 2 b)-h). In Figure 2 g) and h) the residual anomalies using a band pass Butterworth filter wavelength of 20-50 and 40-100 km, respectively, are presented.

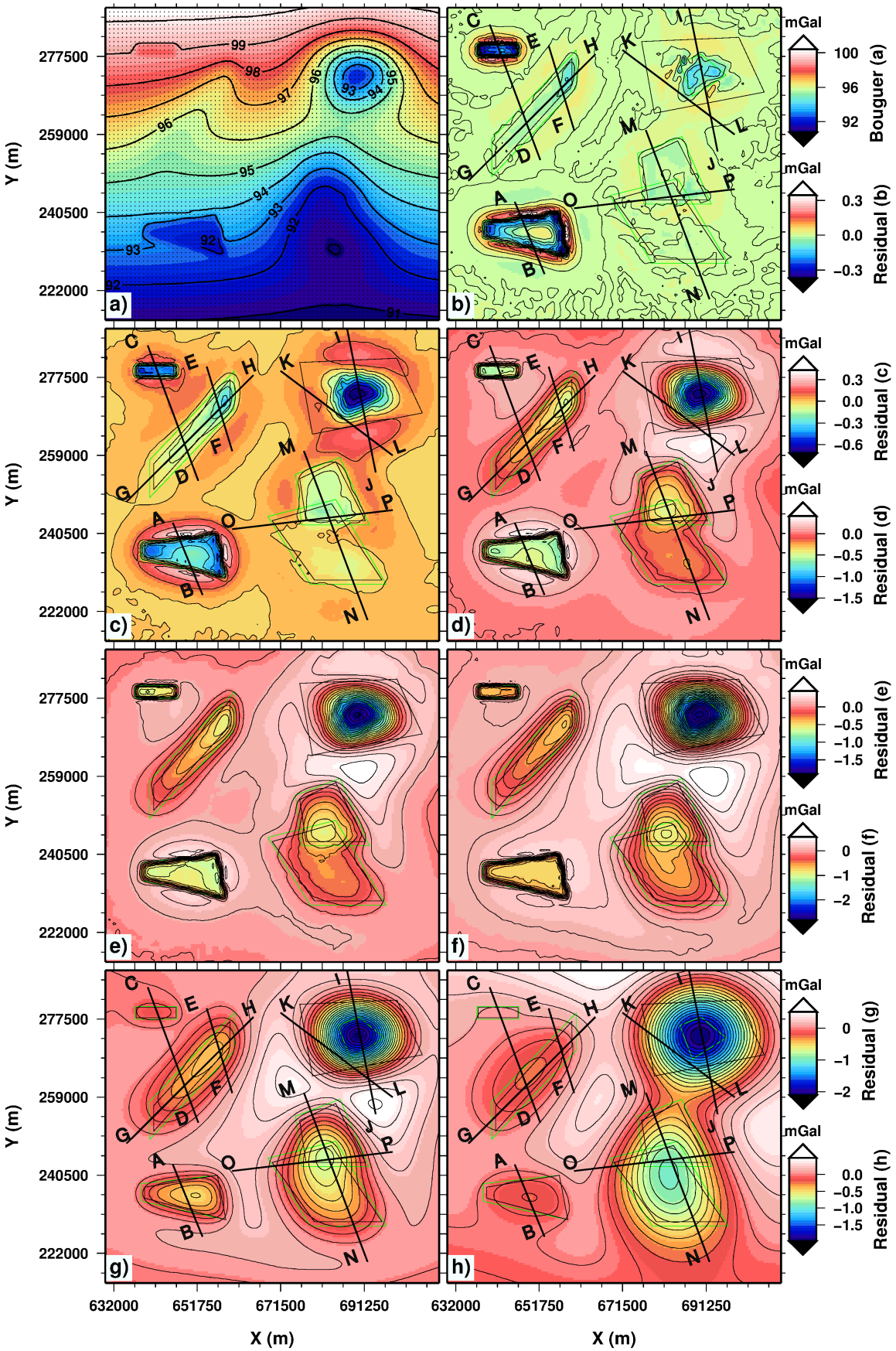

Figure 2: Bouguer and residual anomalies calculated from the synthetic 3D geological model (Figure 1) using density values from Table 1. a) Bouguer anomaly, b) to f) residual anomalies using high-pass Butterworth filters of 0, 20, 30, 35 and 50 km wavelength, respectively, g) and h) residual anomalies using of band-pass Butterworth filter of 20-50 and 40-100 km wavelength, respectively. Lines A-B, C-D, to, O-P indicate the extracted 2D sections presented in Figure 3. The X-Y geometry of the volumes B1 to B6 is shown by green (extension at top) and black lines (extension at bottom).

As expected the 10 km high-pass Butterworth filter (Figure 2 b) reveals clear geometrical outlines for the anomalies B1 and B6. The quality of the outline of the anomalies B4 and the eastern, shallower part of B3 and the top of B2 with respect to the outline of the volume is reduced. The deep parts of B2 and B5 are not recognized in their extension. The dynamic of the residual anomalies ranges between 0.31 and -0.32 mgal and regional trend observed in the Bouguer anomaly appears to be removed completely from the anomaly (Figure 2 b-f). With increasing wavelength of the filter towards higher values the dynamic increases successively up to 2 mgal and the absolute values decrease to 0 to -2.8 mgal for the 50 km filter wavelength. Increasing wavelength sharpens the geometric outline of the shallow volumes B1 and B6 as well as the deeper parts of B2 and B3. A clear separation between B4 and B5 cannot be achieved from the isoline plot using the given range of wavelength. Cutting off the high frequencies seems to introduce again part of the regional signal removed by the high-pass filter (Figure 2 g and h). The accuracy of the outline of the shallow volumes decreases with increasing lower wavelength and the contribution from the deep parts of the volumes becomes more prominent. This is evident, for example, for B5. A separation between B4 and B5 is still not evident from the isoline plot. In order to emphasize the potential in determination of the geometry of the volumes using pseudo-tomography, we present eight 2D profiles through the volumes for the following filters: 10, 20 and 30 km high-pass and 20-50 and 40-100 km band pass filters. The lines A-B, C-D, to, O-P (Figure 2) show the localization of the extracted 2D sections presented in Figure 3.

Cross-section A-B across volume B6 reveals an increase in the amplitude of the anomaly from 10 to 30 km high-pass filter. The negative amplitude of the band-pass filter of 20-50 km is comparable to the latter, whereas the negative amplitude of the 40-100 km filter decreases significantly. This indicates that, as expected, the contribution from shallow depth is dominant. Positive anomalies at the rim of the volume are found only in the high-pass filters. In both type of filters differences of the radius of influence of the anomaly can be observed. The minimum broadens with increasing maximum wavelength. The sharp geometry of the high-pass filtered residual anomalies may even indicate the broadening of the volume with depth. As B1, the volume B6 geologically represents shallow Quaternary sediment that are not of geothermal interest.

The sections I-J and K-L cross the volume B2 in the middle and at a lateral position, respectively. For both profiles, the high-pass filter with a wavelength of 10 km does not show a significant contribution to the residual anomaly of this volume. Starting from a wavelength of 20 km the amplitude increases continuously with increasing maximum wavelength for both profiles with the exception of the amplitude of the band-pass filter 40-100 km for the cross-section I-J that is comparable to the 20-50 km bandwidth. The dynamic of the residual anomalies for the central cross-section I-J is twice the one of the lateral profile K-L. The general increase in amplitude is more prominent for the central position and in particular for the high-pass filters with shorter wavelength. The shallowest part of the volume in the central part of the volume B2 is affected by the 40-100 km band-pass filter causing a reduction in amplitude with respect to the 20-50 km filter. Our observations demonstrated that this type of geometry can be assessed using different wavelength. Geologically, this volume B2 with a relative density difference of 50 kg m^{-3} corresponds to a typical pluton intrusion into the basement. Examples for such type of anomalies and their geothermal relevance are provided in Baillieux et al. (in press).

Geometrically the above discussed profile I-J reveals similarities with the profile E-F cross-cutting the thin inclined volume B3. The dynamic of the residual anomaly, however, is four times larger. The effect of inclination is clearly visible in the profile G-H by its asymmetry as well as in the relative amplitudes in the profiles C-D and E-F, in particular for the band-pass wavelength of 40-100 km. As expected, differences between the band-pass and high-pass filters are largest at the shallow part of the volume. Geologically this volume B3 corresponds to a fault zone with a fracture porosity of a few percent and of shallow inclination.

As described above the most challenging issue in this synthetic model is the separation of the two volumes B4 and B5, since they appear as single anomaly in the isoline plots of all filters (Figure 2). Indication of two distinct volumes can be found applying the high-pass 20 and 30 km filters. This becomes more evident in the profile M-N crossing in approximately N-S direction the two volumes. It can be observed that the amplitude of the two filters is larger for B4 which is located at shallower depth compared to B5. The low amplitude on the B5 volume in these filters as well as the lateral shift in the maximum negative amplitude of the band-pass filters towards B5 indicates that this volume creates a contribution to the residual anomaly from greater depth. Geologically, these two volumes correspond to graben structures situated at the top of the crystalline basement that occur at different depth due to the deepening of the Mesozoic sediments. According to thermo-hydraulic modelling, they are mainly contributing to one of the largest heat flow anomalies in Northern Switzerland (Rybach et al., 1987; Schill et al., 2011).

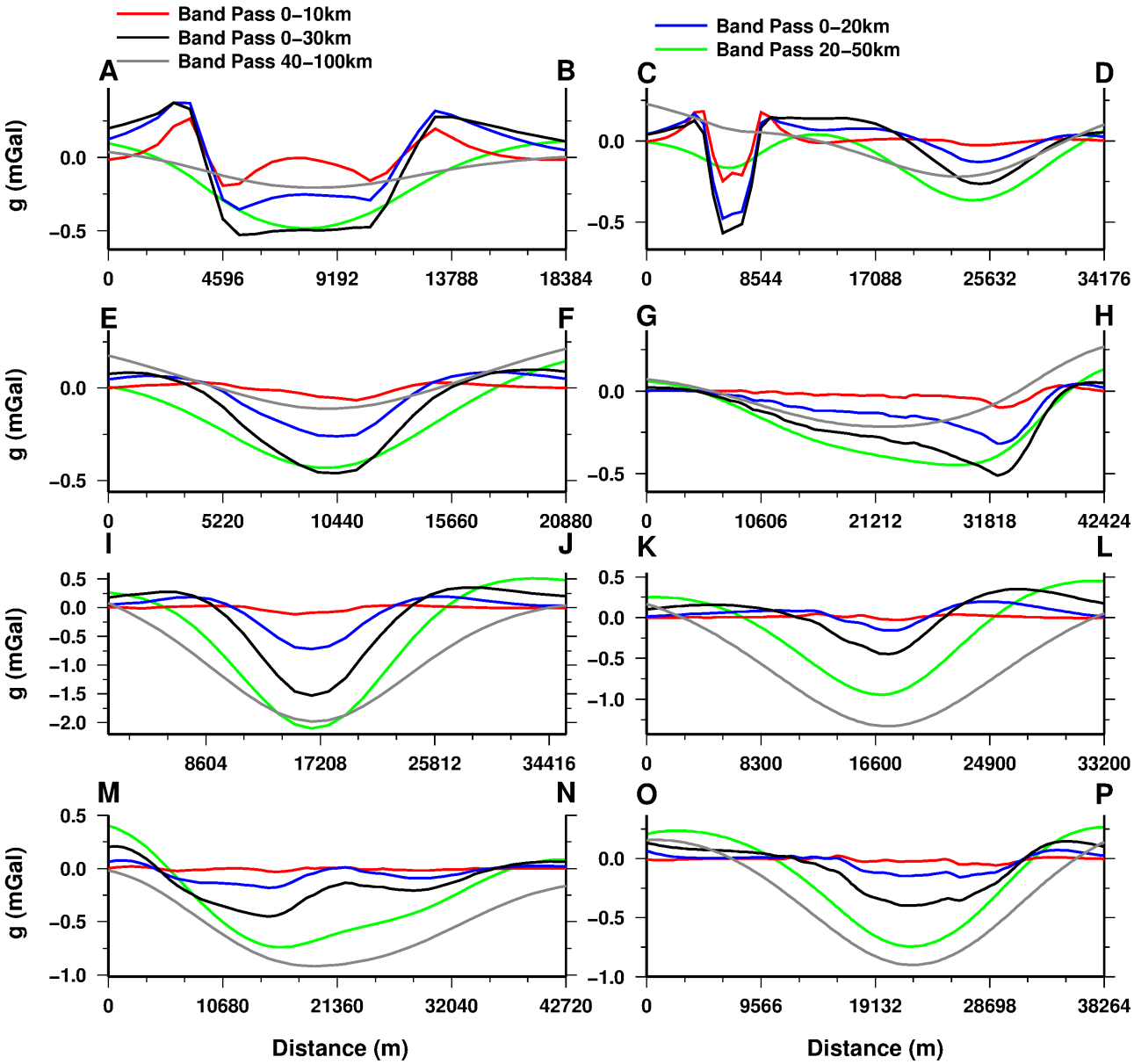

Figure 3: 2D profiles of Bouguer and residual anomalies calculated from the synthetic 3D geological model (Figure 1) using density values from Table 1. Location of the profiles is shown in Figure 2.

5. CONCLUSIONS

In this study, we have presented a sensitivity analysis of Butterworth high-pass and band-pass filters with different wavelength. Furthermore, we have developed numerical forward modelling software based on 3D geological FE models. The following conclusions can be drawn from this study:

1) Quaternary sediments can be located and well delimited in their extension using short-wavelength high-pass filters. Band-pass filters may be used to erase the majority of their contribution to the gravity signal, since they are not of geothermal significance.

2) Variation in the basement lithology can be geometrically described in detail at their top and with acceptable accuracy at their bottom using high-pass and band-pass filters, respectively. Changes in basement lithology mainly contribute to geothermal anomalies in terms of changes in heat production (Baillieux et al., in press).

3) Fault zones in the basement with shallow inclination can be described geometrically, when a density contrast ranges in the order of about 70 kg m^{-3}. This corresponds to fracture porosity in the fault zone of a few percent. Such fault zones can offer fluid path ways for hydrothermal circulation.

4) Tracing graben structures in the Variscian basement of Switzerland known as Permo-Carboniferous troughs is a major challenge in the area of heat flow anomalies in Switzerland. Our sensitivity study shows that wavelength dependent Butterworth filtering in combination with 3D forward modelling based on FE discretized geological models is a powerful tool to locate and comprehend those structures in their 3D extension.

Furthermore, we would like to point out that first results from real data in a test area in Northern Switzerland confirm our observations in the sensitivity study.

ACKNOWLEDGEMENTS

We would like to thank swisstopo and the Swiss Geophysical Commission for providing topographic data as well as gravity data for first tests. P. Kuhn kindly contributed to the geological discussion.

REFERENCES

Abdelfettah Y. & Schill E.: Delineation of geothermally relevant Paleozoic graben structures in the crystalline basement of Switzerland using gravity. Society of Exploration Geophysics meeting, Proceeding, Istanbul, 2012

Baillieux, P., Schill, E., Edel, J.-B., Mauri, G.: Localization of temperature anomalies in the Upper Rhine Graben: insights from geophysics and neotectonic activity, *International Geology Review*, (in press).

Allenbach R. P. and A. Wetzel, 2006. Spatial patterns of Mesozoic facies relationships and the age of the Rhenish Lineament: a compilation, Int J Earth Sci (Geol Rundsch), 95, 803-813. DOI 10.1007/s00531-006-0071-0

Bächler, D., 2003. Coupled Thermal-hydraulicchemical modeling at the Soultz-sous-Forêts HDR reservoir (France). PhD, Swiss Federal Institute of Technology.

Boigk, H., and H. Schöneich, 1970. Die Tiefenlage der Permbasis im nördlichen Oberhreingraben. in International rift symposium Graben Problems, eds Illies, J. H. & Müller, S. E. Schweizerbart'sche, Karlsruhe.

Boigk, H., and H. Schöneich, 1974. Perm, Trias und älterer Jura im Bereich der südlichen Mittelmeer-Mjösen-Zonen und des Rheingrabens. in International rift symposium: Approaches to Taphrogenesis, eds Illies, J. H. & Fuchs, K. Schweizerbart'sche, Karlsruhe.

Butterworth, S., 1930. On the theory of filter amplifiers. Wireless Engineering, 1: 536-541.

Diebold, P., H. Naef and M. Ammann, 1991. Zur Tektonik der zentralen Nordschweiz: Interpretation aufgrund regionaler Seismik, Oberflächengeologie und Tiefbohrungen. in Technischer Bericht, ed NAGRA. Nagra, Wettingen.

Diebold, P. and T. Noack, 1997. Late Paleozoic troughs and Tertiary structures in the eastern folded Jura. In: O.A. Pfiffner, P. Lehner, P. Heitzmann, S. Mueller and A. Steck (Editors), Deep structure of the Swiss Alps. Birkhäuser Verlag, Basel.

Geuzaine C. and J.-F. Remacle, 2009. Gmsh: a three-dimensional finite element mesh generator with built-in pre- and post-processing facilities. International Journal for Numerical Methods in Engineering, Volume 79, Issue 11, pages 1309-1331.

Gorin, G.E., C. Signer and G. Amberger, 1993. Structural configuration of the western Swiss Molasse basin as defined by reflection seismic data, Eclogae geol. Helv., 86, 693-716.

Illies, H.J. and G. Greiner, 1979. Holocene movements and state of stress in the rhinegraben rift system. Tectonophysics, 52(1-4): 349-359.

Klingelé, E. and H. Schwendener, 1984. Geophysikalisches Untersuchungsprogramm Nordschweiz: Gravimetrische Messungen 81/82, Nagra, Baden.

Kohl, T., D. Bächler and L. Rybach, 2000. Steps towards a comprehensive thermo-hydraulic

analysis of the HDR test site Soultz-sous- Forêts. Proc. World Geothermal Congress 2000, Kyushu-Tohoku, Japan, May–June 2000, pp. 2671–2676.

Laubscher, H. and T. Noack, 1997. The deep structure of the Basel Jura. in Deep Structure of the Swiss Alps, pp. 54-58, eds. Pfiffner, O. A., Lehner, P., Heitzmann, P., Müller, S. & Steck, A. Birkhäuser, Basel.

Marchant, R., Y. Ringgenberg, G. Stampfli, P. Birkhäuser, P. Roth and B. Meier, 2005. Paleotectonic evolution of the Zürcher Weinland (northern Switzerland), based on 2D and 3D seismic data, Eclogae geologica Helvetica, 98, 345-362.

Matter, A., Peters, T., Isenschmid, C., Bläsi, H.-R. and Ziegler, H.-J., 1987. Sondierbohrung Riniken - Geologie. Nagra Technische Berichte, NTB 86-02: 1-200.

NAGRA, 2008. Vorschlag geologischer Standortgebiete für das SMA- und das HAA-Lager - Geologische Grundlagen. in Technischer Bericht 08-04, ed Nagra. Nagra, Wettingen.

Pfiffner, O.A., P. Erard and M. Stäuble, 1997. Two cross sections through the Swiss Molasse Basin (lines E4-E6, W1, W7-W10). in Deep Structure of the Swiss Alps: Results of NRP 20, pp. 64-72, eds. Pfiffner, O. A., Lehner, P., Heitzmann, P., Müller, S. & Steck, A. Birkhäuser, Basel.

Pohanka V., 1988. Optimum expression for computation of the gravity field of a homogeneous polyhedral body. Geophysical Prospecting 36, 733-75.

Pribnow, D. and R. Schellschmidt, 2000. "Thermal tracking of upper crustal fluid flow in the Rhine Graben." Geophysical Research Letters 27(13): 1957-1960.

Rybach, L., Eugster, W. and Griesser, J.C., 1987. Die geothermischen Verhaeltnisse in der Nordschweiz. Eclogae geol. Helv., 80(2): 521-534.

Schill E., T. Kohl, J. Geiermann, C. Baujard, S. Koch, H. Deckert, G. Munoz, Y. Abdelfettah, 2011. Multi-disciplinary prospection approach for EGS reservoirs in the german variscian basement. Proceedings, Thirty-Sixth Workshop on Geothermal Reservoir Engineering Stanford University, Stanford, California, SGP-TR-191 January 31 - February 2, 2011.

Schill, E., Guglielmetti, L., Klingler, P., Abdelfettah, Y., Alcolea, A., 2012: The role of structural changes for geothermal projects in the area of Basel *Proceedings of the Thirty-Seventh Workshop on Geothermal Reservoir Engineering*, , Stanford, California, SGP-TR-194.

Sommaruga A., U. Eichenberger and F. Marillier, 2012. Seismic Atlas of the Swiss Molasse Basin. 24 Tafeln. ISBN 978-3-302-40064-8.

Sprecher C. and W.H. Müller, 1986. Geophysikalisches Untersuchungsprogramm Nordschweiz: Reflexionsseismik 82, Nagra NTB 84-15.

Ustaszewski, K.M., 2004. Reactivation of pre-existing crustal discontinuities; the Southern Upper Rhine Graben and the Northern Jura Mountains: a natural laboratory, University of Basel.